Parietal lobe variation in cercopithecid endocasts

Ana Sofia Pereira-Pedro[1], Amélie Beaudet[2,3] and Emiliano Bruner[1]

[1]Programa de Paleobiología, Centro Nacional de Investigación sobre la Evolución Humana, Burgos, Spain

[2]School of Geography, Archaeology and Environmental Studies, University of the Witwatersrand, Johannesburg, South Africa

[3]Department of Anatomy, University of Pretoria, Pretoria, South Africa

* Correspondence to: Ana Sofia Pereira-Pedro, Centro Nacional de Investigación sobre la Evolución Humana, Paseo Sierra de Atapuerca 3, 09002 Burgos, Spain. Email: sofia.aspp@gmail.com

Abstract

In extant primates, the posterior parietal cortex is involved in visuospatial integration, attention, and eye-hand coordination, which are crucial functions for foraging and feeding behaviors. Paleoneurology studies brain evolution through the analysis of endocasts, that is molds of the inner surface of the braincase. These may preserve imprints of cortical structures, such as sulci, which might be of interest for locating the boundaries of major cortical regions. Old World monkeys (Cercopithecidae) represent an interesting zoological group for evolutionary studies, because of their diverse ecologies and locomotor behaviors. In this study, we quantify parietal lobe variation within the cercopithecid family, in a sample of 30 endocasts including 11 genera and 17 species, by combining landmark-based and landmark-free geometric morphometric analyses. More specifically, we quantitatively assess variation of the parietal proportions based on landmarks placed on reliable anatomical references and of parietal lobe surface morphology through deformation-based methods. The main feature associated with the cercopithecid endocranial variation regards the inverse proportions of parietal and occipital lobes, with colobines, *Theropithecus*, and *Papio* displaying relatively larger parietal lobes and smaller occipital lobes compared with cercopithecins. The parietal surface is anteroposteriorly longer and mediolaterally flatter in colobines, while longitudinally shorter but laterally bulging in baboons. Large parietal lobes in colobines and baboons are likely to be independent evolutionary traits, and not necessarily associated with analogous functions or morphogenetic mechanisms.

KEYWORDS

geometric morphometrics, Old World monkeys, parietal cortex, sulcal patterns, surface-based analysis

HIGHLIGHTS

- Sulcal imprints on the surface of cercopithecid endocranial casts have shown differences between the two subfamilies, cercopithecinae and colobinae.
- Landmark-based analysis allowed a quantification of these differences, confirming colobines have proportionately larger parietal lobes.
- *Theropithecus* and *Papio* display colobine-like proportions.
- Colobuses and baboons evolved a larger parietal cortex through distinct mechanisms.

1. INTRODUCTION

In primates, parietal lobes generally include the anterior parietal cortex, which mainly deals with somatosensory functions, and the posterior parietal cortex (PPC), which is a major associative region of the mammalian brain (Whitlock, 2017). The PPC receives multiple stimuli from sensorimotor, visual, and auditory systems, including information on spatial properties, motion, location, and orientation of objects, and integrate proprioceptive feedbacks for planning actions, such as eye saccades and visual fixation, or hand movements for reaching (reviewed in Grefkes & Fink, 2005). Furthermore, the PPC is also involved in attention, spatial navigation, and memory, and it has been suggested that its evolution in primates is influenced by explorative and feeding behaviors (Goldring & Krubitzer, 2017). In primates, the eyes and the hands are the main interfaces between brain and environment, and the processes of visuospatial integration that include body cognition and spatial perception, visual imagery and simulation, and eye-hand coordination, are directly involved in the evolution of the PPC (Bruner & Iriki, 2016). Eye-hand coordination is particularly important in the sense that reaching, grasping, and bringing food items to the mouth could have been the major selective force acting on the evolution of the PPC, a region that has increased in terms of size and complexity in primates, especially in humans (Goldring & Krubitzer, 2017). Indeed, the parietal lobes of modern humans are larger when compared with other living apes and to extinct human species, suggesting that regions within the PPC underwent expansion and reorganization in association with human-specific cognitive functions, such as tool use (Bruner, 2018; Catani et al., 2017; Kastner, Chen, Jeong, & Mruczek, 2017). However, in neurosciences, parietal cortical anatomy in primates has been mainly investigated in terms of cytoarchitecture, and data available mainly concern humans and macaques. Accordingly, despite the pivotal role of the parietal lobe in the evolution of primate brain and behavior, evidence documenting the cortical anatomy of the parietal region is relatively scarce or even absent for most of the primate taxa.

The Old World monkeys (superfamily Cercopithecoidea, family Cercopithecidae) represent a large primate group encompassing African and Asian species and spanning a variety of habitats, diets, body sizes, and social organizations. Connolly (1950), in his monograph, observed that their sulcal patterns were fairly uniform, though the two subfamilies differed regarding the relative location of the lunate sulcus, so Colobinae have larger parietal lobes while Cercopithecinae have larger occipital lobes. The description of fossil endocasts, i.e., molds of the inner surface of the braincase, provides additional evidence for discussing brain evolution in the different cercopithecoid lineages. In particular, Radinsky (1974) suggested that the cercopithecine sulcal pattern is derived as compared with that of the colobines, as the latter display some of the features of the prosimian pattern (i.e., smaller occipital lobes, and a

similar course of the intraparietal sulcus to its prosimian homolog; Radinsky, 1974). Falk (1978) further described the differences in the sulcal patterns of cercopithecines and colobines, analyzing the endocasts of extant genera. For instance, cercopithecines display convergent Sylvian fissure and superior temporal sulcus, and relatively straight intraparietal and lunate sulci, while in colobines the first two sulci are parallel and the latter two are relatively arched (see Falk, 1978). The cited studies emphasize the endocasts' value for localizing boundaries and cortical proportions of the main cerebral regions through the examination of the sulcal references. Besides the description of sulcal patterns, the observed sulcal imprints could be useful for quantitative analysis through geometric morphometrics. Nonetheless, as endocasts only display partial information of the anatomical details, the use of landmarks based on brain structures is scarcely used (Neubauer, 2014; Pereira-Pedro & Bruner, 2018). On the other hand, it has been shown that sulcal patterns are easier to recognize on smaller endocasts, such as those of macaques because imprints are more marked and probably also because the sulcal schemes are simpler (Kobayashi et al., 2014; Van Minh & Hamada, 2017). In this context, Old World monkeys could be useful for analyses of lobe proportions, as sulcal imprints not only can be identified on their endocasts but have also been extensively studied and described.

More recently, new methods based on surface deformation are emerging in the effort to overcome problems associated with correspondence and localization of landmarks (Dupej et al., 2018; Durrleman, Pennec, Trouvé, Ayache, & Braga, 2012). Beaudet et al. (2016) applied landmark-free surface deformation methods, coupled with automatic detection of sulcal patterns, for quantifying the shape variation in cercopithecoid endocasts. They analyzed South African cercopithecoid fossil endocasts comparatively to the extant taxa, with a particular interest in *Theropithecus* subspecies and *Cercopithecoides williamsi*. The deformation methods subdivided the extant sample into groups corresponding to the main cercopithecid tribes—papionini, cercopithecini, and colobini. Regarding the cercopithecoid fossils, they observed that the fossil colobine *C. williamsi* displayed relative endocranial volume and sulcal pattern similar to papionins and that the sulcal pattern of fossil *Theropithecus* varies across subspecies and differs between the extinct and extant species (Beaudet et al., 2016).

In this study, we quantitatively describe the variation of the parietal lobe in extant cercopithecid endocasts through the use of imaging techniques and geometrical models. First, we use landmark-based geometric morphometric analysis to describe variation in the relative proportions of the parietal lobe, as previously reported by Radinsky (1974) and Falk (1978) based on visual inspection of endocasts. Second, we apply deformation-based models to the endocast's parietal lobe surface to further characterize parietal-only morphological variation. Considering the previously reported differences in the relative position of the lunate sulcus between the two subfamilies (Connolly, 1950; Falk, 1978; Radinsky, 1974), we expect the parietal lobes to be proportionally larger in colobines than in cercopithecines. Regarding morphological variation, we compare the parietal morphology in colobines and cercopithecines under the null hypothesis of no shape differences. By combining the two methods, we aim to provide a complementary analysis of the parietal morphology both in terms of overall form and localized variation.

2. METHODS

This study was performed on virtual endocasts from previous studies and online collections (see below). The research complies with the American Society of Primatologists Principles

for the Ethical Treatment of Nonhuman Primates, protocols of the appropriate Institutional Animal Care Committee, and legal requirements of each country housing collections.

2.1. Sample

We follow the taxonomy adopted by Grubb et al. (2003). Our sample includes 30 cercopithecid endocasts spanning 11 genera and 17 species (Table 1). The specimens are all considered adult, according to teeth eruption. Sex differences are not considered in this study. The endocasts from most specimens have been reconstructed and analyzed previously in Beaudet et al. (2016). For the present work, we added three more specimens downloaded from the online platform MorphoSource (www.morphosource.org). These include two *Cercocebus torquatus* housed at the Museum of Comparative Zoology, Harvard University (Cambridge, MA), and digitized by Copes, Lucas, Thostenson, Hoekstra, and Boyer (2016) and one *Theropithecus gelada* from the Delson Primate Scans Project and the American Museum of Natural History (New York, NY). The virtual endocasts of these three specimens were digitally reconstructed by using the Endex software (Subsol, Gesquière, Braga, & Thackeray, 2010).

Table 1. Cercopithecoid taxa and repositories

Genus	Species	N	Repository
Colobinae (colobines)			
Colobus	*C. guereza*	6	MRAC; AMNH; MNHN
Piliocolobus	*P. foai*	1	MRAC
Cercopithecinae (cercopithecines)			
Cercopithecini (cercopithecins)			
Cercopithecus	*C. cephus*	2	MHNT
Chlorocebus	*C. aethiops*	2	MHNT
	C. pygerythrus	2	MRAC
Erythrocebus	*E. patas*	1	MHNT
Papionini (papionins)			
Cercocebus	*C. atys*	1	MRAC
	C. turquatus	2	MCZ
Lophocebus	*L. albigena*	2	MRAC; MNHN
Macaca	*M. mulatta*	1	MHNT
	M. sylvanus	1	MHNT
Mandrillus	*M. leucophaeus*	2	MRAC
Papio	*P. anubis*	1	MNHN
	P. cynocephalus kindae	1	MRAC
	P. hamadryas	1	MNHN
	P. ursinus	1	MNHN
Theropithecus	*T. gelada*	3	AMNH; MNHN

Note: Taxonomy based on Grubb et al. (2003).
Abbreviations: AMNH, American Museum of Natural History, New York; MCZ, Museum of Comparative Zoology, Harvard University; MNHN, Muséum National d'Histoire Naturelle, Paris; MHNT, Muséum d'Histoire Naturelle de Toulouse; MRAC, Musée royal de l'Afrique centrale, Tervuren.

2.2. Landmark analysis

We chose a set of 25 anatomical landmarks largely based on the cortical sulci that can be observed in the cercopithecoid endocasts (Figure 1 and Table 2). On the midsagittal contour, we placed three landmarks defining the boundaries between the parietal, occipital, and cerebellar regions ($CS_{(mid)}$, POB, and IOP). The other 22 landmarks were located on both hemispheres (11 each), and are either outmost points of the endocast (FP, OP, TP, CP, and BC) or limits or midpoints of the main sulci (IPS, $CS_{(lat)}$, SF, LU, AS, and PCS).

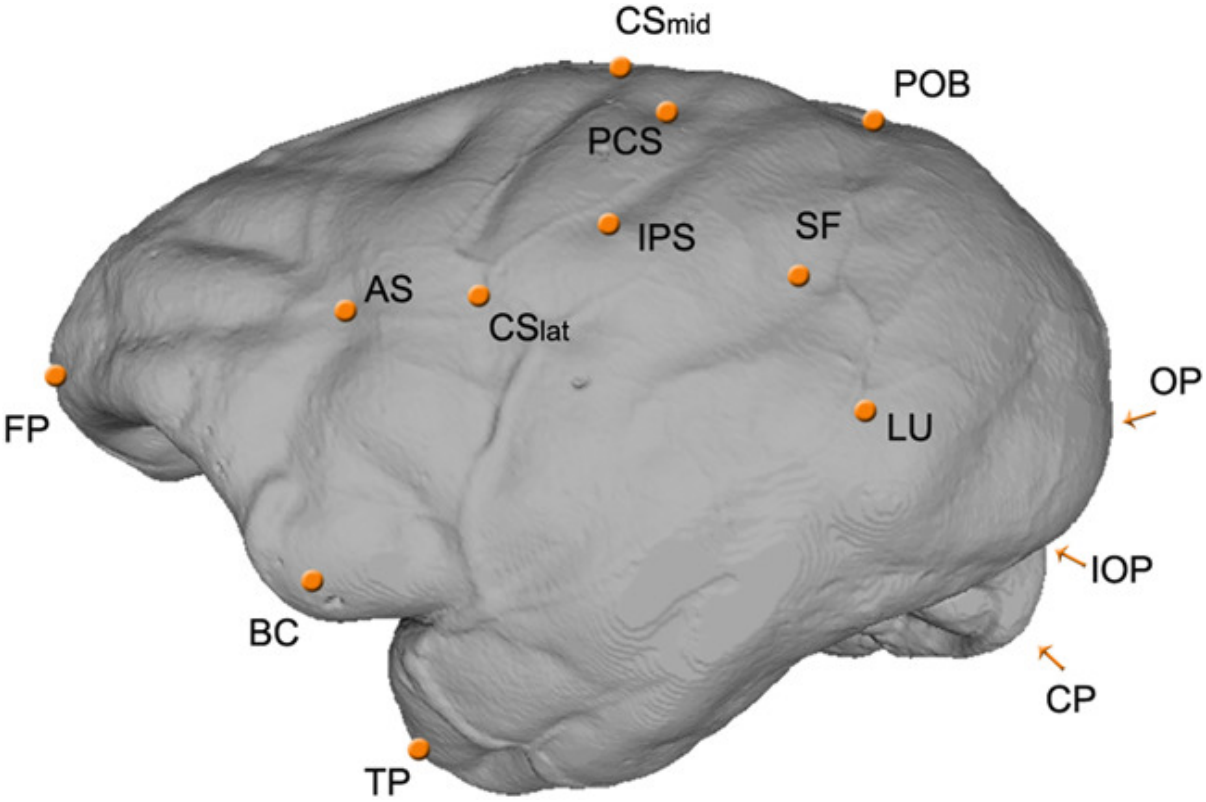

Figure 1.. Anatomical landmarks used for the geometric morphometrics analysis: AS, arcuate sulcus; BC, Broca's cap; CP, cerebellar pole; $CS_{(lat)}$, central sulcus (lateral); $CS_{(mid)}$, central sulcus (midsagittal); FP, frontal pole; IOP, internal occipital protuberance; IPS, intraparietal sulcus; LU, lunate sulcus; OP, occipital pole; PCS, postcentral notch; POB, parietooccipital boundary; SF, Sylvian fissure; TP, temporal pole. See Table 2 for the definition of the landmarks. Specimen: *Chlorocebus aethiops*, Cercopithecini, Cercopithecinae

Table 2. Anatomical landmarks and definitions

Landmark	Meaning	Location
$CS_{(mid)}$	Central sulcus (midsagittal)	Point of intersection of the central sulcus with the midline
POB	Parieto-occipital boundary	Point of intersection of the lunate sulcus with the midline
IOP	Internal occipital protuberance	Point of intersection of the four divisions of the cruciform eminence
FP	Frontal pole	Anterior most point; point of maximum curvature
OP	Occipital pole	Posterior most point; point of maximum curvature
TP	Temporal pole	Anterior end of temporal lobe; point of maximum curvature
CP	Cerebellar pole	Outmost point; point of maximum curvature
BC	Broca's cap	Point of maximal width on the frontal region homologous to human Broca's area
AS	Arcuate sulcus	Point of maximal bending, following the length of the frontal sulcus
$CS_{(lat)}$	Central sulcus (lateral)	Inferior limit of the central sulcus
PCS	Postcentral notch	A point of depression anterior and superior to the Intraparietal sulcus
IPS	Intraparietal sulcus	Inferior limit of the intraparietal sulcus
SF	Sylvian fissure	Posterior limit of the Sylvian fissure/lateral sulcus
LU	Lunate sulcus	Inferior limit of the lunate sulcus

Landmarks were digitized in threedimensions using Landmark Editor (IDAV), and geometric morphometric analysis was performed with PAST v2.17c (Hammer, Ryan, & Harper, 2001) and MorphoJ v1.6b (Klingenberg, 2011). Landmarks were registered by Procrustes superimposition, which normalizes the information on size, position, and orientation (Zelditch, Swiderski, Sheets, & Fink, 2004). Configurations were symmetrized, averaging right and left hemispheres (Klingenberg, Barluenga, & Meyer, 2002). The number of individuals for each species does not allow a proper survey of the specific or intraspecific variation and, accordingly, we performed the analysis averaging the values for each genus. After registering the coordinates, the main patterns of variation were analyzed through Principal Component Analysis (PCA; Jolliffe, 2002; Zelditch et al., 2004) to identify the main shape differences among the genera. Allometry was tested by the correlation between shape coordinates and endocranial volumes. We used a two-tailed significance level of 0.05. In addition, we computed a cluster analysis by unweighted pair-group average (UPGMA) on the registered coordinates, to quantify the degree of morphological affinity between genera.

2.3. Extraction of the parietal surface

To analyze the variation of the parietal surface only, we first had to define its limits on the endocasts for subsequent virtual separation from the rest of the endocranial surface (as in Beaudet & Bruner, 2017 for the frontal lobes). Based on previous works (Falk, 1978; Radinsky, 1974), we used the central sulcus as the anterior limit of the parietal lobe, and the lunate sulcus as its posterior limit. For the inferior limit, we used the Sylvian fissure, which roughly separates the parietal lobe from the temporal lobe, at least in its anterior region. However, as these anatomical references are not always visible on endocasts, we tentatively defined the parietal limits in terms of general geometric references. The inferior parietal limits correspond to a plane defined by two landmarks placed on the inferior point of the central sulcus and on the posterior point of the Sylvian fissure of both hemispheres. The posterior limits correspond to a plane defined by four landmarks located on the left and right lunate sulci, two of them intersecting the previous plane. The anterior and superior borders correspond to the central sulcus and interhemispheric scissure, respectively. The definition of the parietal limits and subsequent extraction of the parietal surfaces was performed with the

software Avizo v9.0. (Visualization Sciences Group Inc.), following the steps illustrated in Figure 2. Two separated parietal surfaces left and right were generated for each specimen.

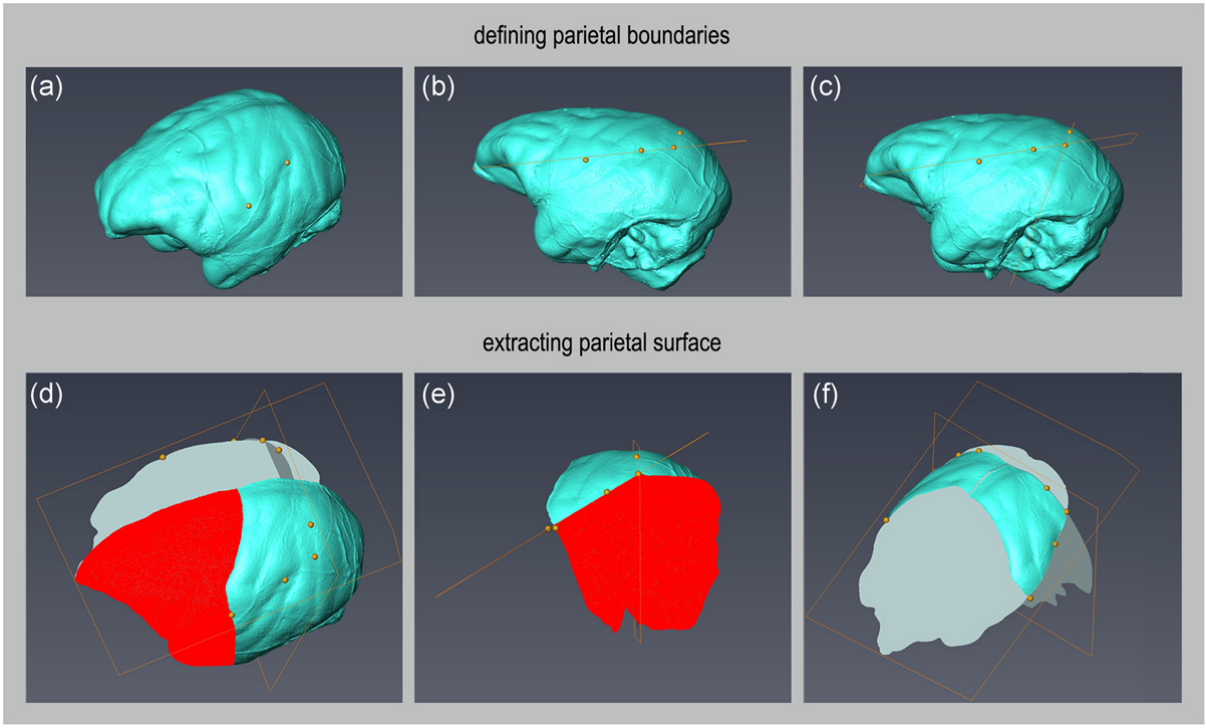

Figure 2. Steps for separating the parietal surfaces from the rest of the endocast: the parietal boundaries are delimited by cross-sections defined by four landmarks placed on both hemispheres (upper panel), and the parietal surface on each hemisphere is extracted by deleting the extra-parietal regions (red areas, lower panel). (a) Location of landmarks on the central sulcus and Sylvian fissure; (b) cross-section defined by the landmarks on (a) and location of the landmarks on the lunate sulcus, which define the cross-section for the posterior border of the parietal (c). After deleting one of the hemispheres, the portion anterior to the central sulcus (red area in d), the portion inferior to the first cross-section (red area in e) and the portion posterior to the second cross-section (not shown) are selected and deleted. This is repeated on the other hemisphere, resulting in two separate parietal surfaces—left and right—for each specimen (f). Note that although shown together, each parietal surface was isolated separately. Specimen: *Macaca mulatta*, Papionini, Cercopithecinae

2.4. Surface deformation methods

The deformation-based models are based on the metric of currents (i.e., a nonparametric representation of shapes as vector fields), which does not assume point-to-point correspondence, allowing for direct comparison of surfaces, measuring the distance between the surfaces as well as the difference between their local orientations (Beaudet & Bruner, 2017; Beaudet et al., 2016; 2018; Durrleman et al., 2012). Following the protocol detailed in Beaudet et al. (2016), endocasts were rigidly aligned in position, orientation, and scale with respect to a reference surface (randomly selected) using the iterative closest point algorithm. A global mean shape (group average) was computed from the set of aligned surfaces and then deformed into each specimen (for further details see Beaudet et al., 2016; 2018; Durrleman et al., 2014). The deformation fields integrating local orientation and the amplitude of the deformations from the global mean shape into each specimen were statistically analyzed through PCA. We consider only the parietal surfaces, analyzing left and right separately. The magnitudes are illustrated by a color code which ranges from dark blue (lowest displacement values) to red (highest displacement values). The computation was performed with the free software Deformetrica (www.deformetrica.org) by using the supercomputer available at the Centre for High-Performance Computing of Cape Town (https://www.chpc.ac.za/).

3. RESULTS

3.1. Landmark analysis

Considering the PCA computed on the genus averages, only the first and second PCs were found to be above the threshold for random variation, explaining 66.5% of the variance. Subsequent PCs were below the threshold of random variation, and will not be considered here (Jolliffe, 2002). The distribution of genera and variation in the endocranial shape described by each component is shown in Figure 3. PC1 accounts for 46.4% of the variance, describing the longitudinal (antero-posterior) proportions of the parietal and occipital lobes. Along with this component, colobines, *Papio*, and *Theropithecus* are distributed toward the positive values, displaying larger parietals and reduced occipitals, while cercopithecines plot toward the negative values and show the opposite proportions. The remaining papionins are distributed in between the cercopithecines and the colobines. PC2 explains 20.2% of the variation in shape, and it is associated with variation in height of the vault, especially on the parieto-occipital region. Colobines are characterized by low and flat braincases while cercopithecines, and particularly the baboons, display comparatively taller vaults.

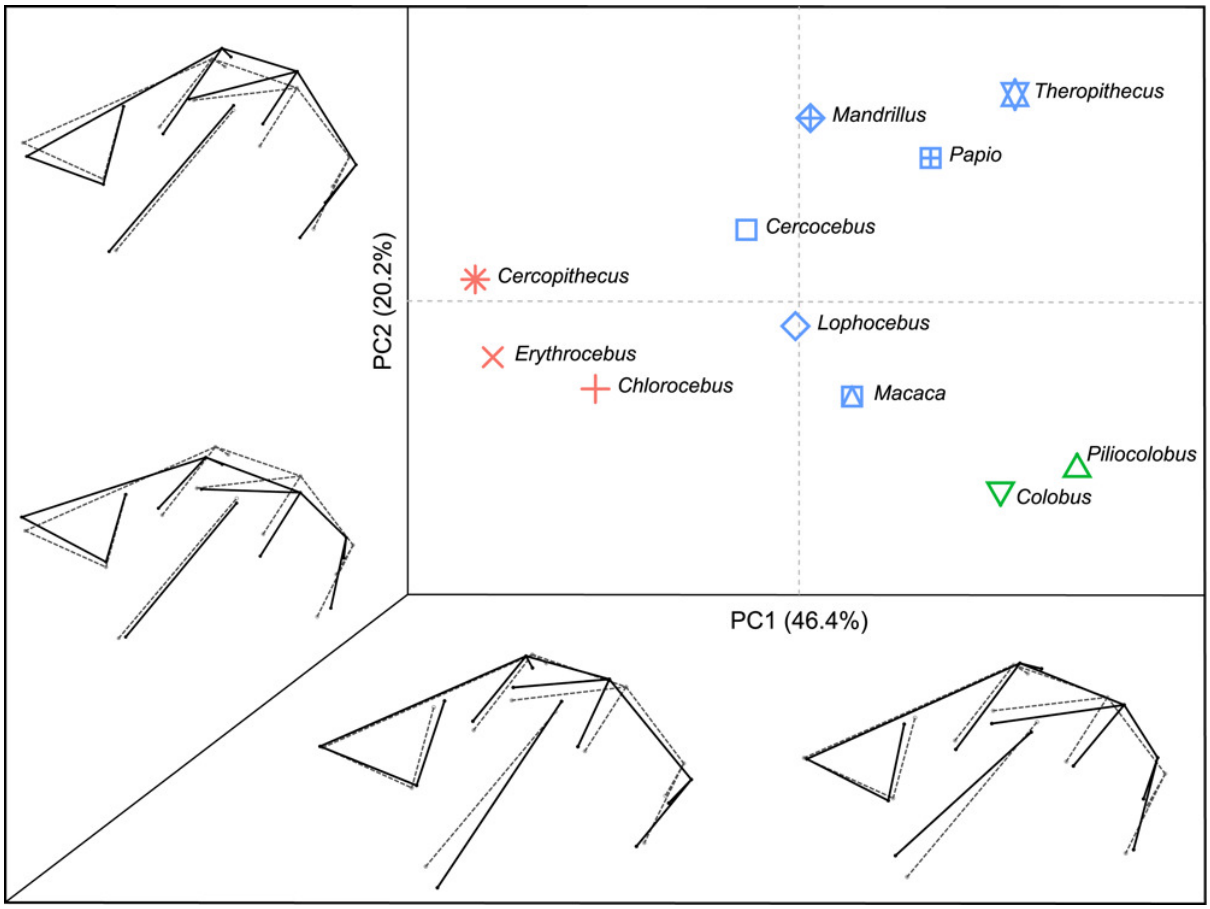

Figure 3. Results from the PCA of the endocast shape according to the landmark analysis. Distribution of specimens on the PC1 vs. PC2 plot and wireframes illustrating the shape changes along each axis. The colors on the PCA plot represent the tribes: red, Cercopithecini; blue, Papionini; and green, Colobini. Wireframes show the mean shape (dashed lines), and the shape variation (continuous lines) towards the negative and positive scores along each PC

To further explore the morphological affinity between the genera, we computed a cluster analysis (UPGMA). The results show that the landmark set used is sufficient to separate the

three tribes and group the different genera (Figure 4). According to the average shapes, Colobini and Papionini are more similar to each other than to Cercopithecini. The three cercopithecini genera display very similar mean shapes. In contrast, the two colobini genera are more distant to each other in terms of morphology. Within the papionins, *Theropithecus* shows the most distinct figure, *Mandrillus* is closer to *Papio*, and *Macaca* groups with the mangabeys.

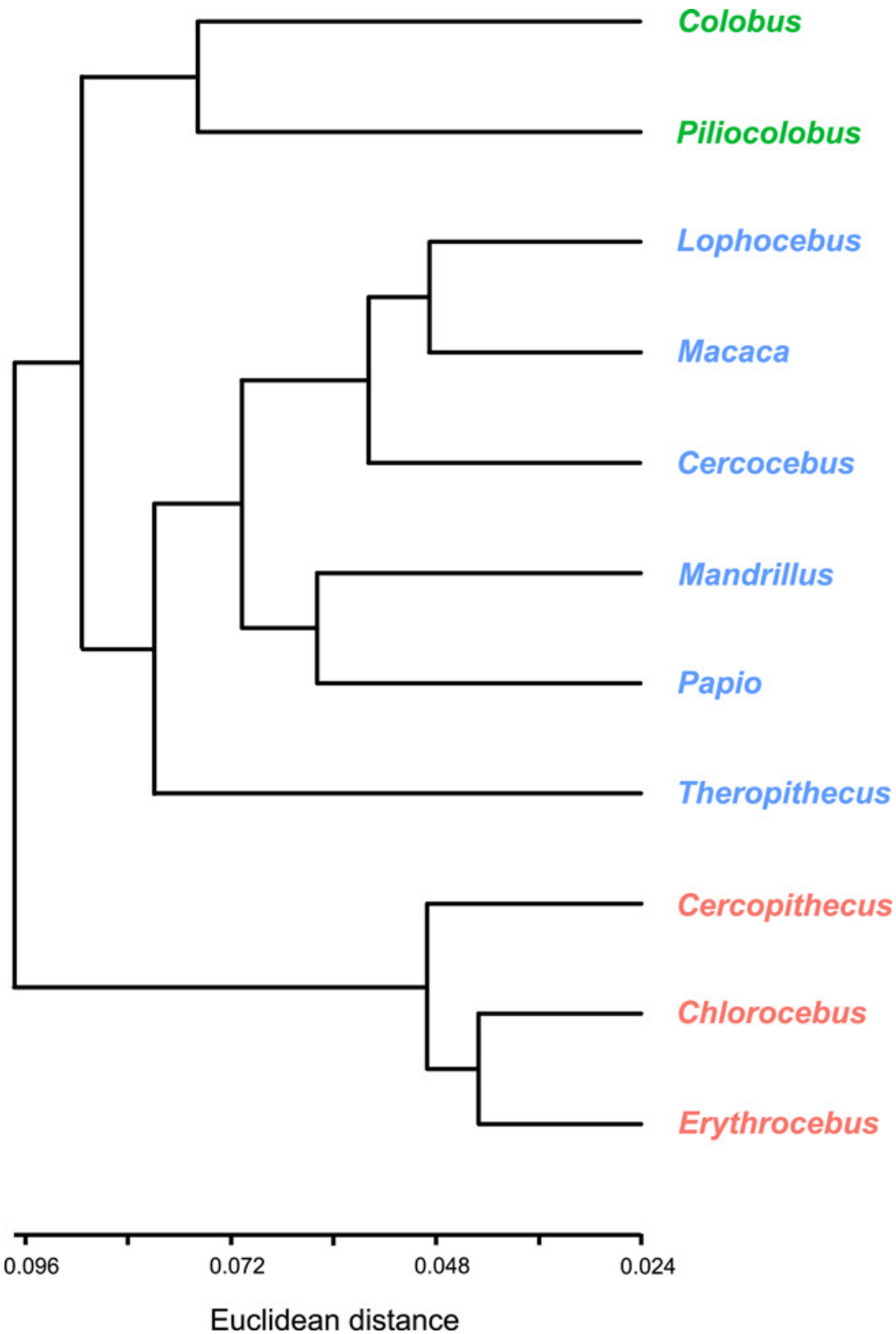

Figure 4. Unweighted pair-group averages computed on the registered (Procrustes) coordinates, showing the shape distances between the genera (Cercopithecini in red, Papionini in blue, and Colobini in green). Cophenetic correlation coefficient = 0.705

The regression of the whole shape with endocranial volume indicates that the variation in the latter explains about 22% ($p \leq .05$) of total shape variation, with the allometric pattern associated with vault height (Figure 5). Endocranial volume is actually correlated with PC2 (68%; $p \leq .05$) but not with PC1 ($p = .23$). In the regression analysis, the colobines and *Theropithecus* depart from the apparent linear trend of the remaining genera.

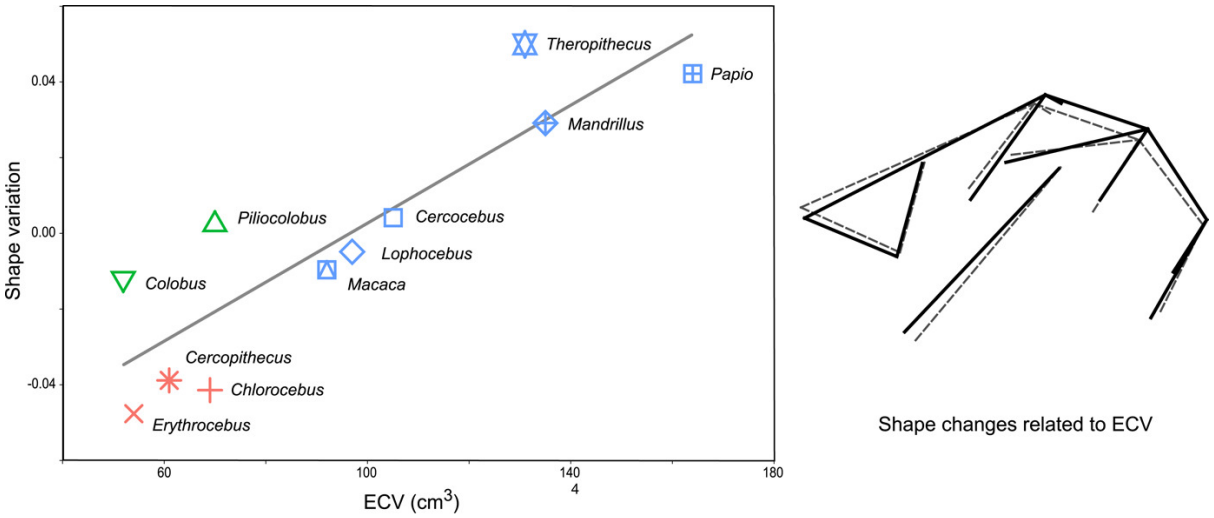

Figure 5. Regression of the whole shape variation on total endocranial volume (ECV): scatter plot (left) and associated shape variation (right). Cercopithecini in red, Papionini in blue, and Colobini in green

3.2. Surface deformation analysis

Figure 6 shows the plots of principal component analyses computed for the left and right parietal surfaces. In both analyses, variation along PC1 is associated with changes in the anteroposterior width of the parietal surface and the shape of the posteroinferior (i.e., the intersection between the lateral and the lunate sulci) and of the anteroinferior (i.e., intersection between the lateral and central sulci) angles. Variation along PC2 is related with changes in anteroposterior width, the shape of the anteroinferior angle, and the degree of inflation of the parietal surface. The distribution of specimens is similar on both PCAs. PC1 mainly separates cercopithecin genera, and *Macaca* and *Cercocebus*, from colobines, *Mandrillus*, *Papio*, and *Theropithecus*. The former group displays a relatively opened posteroinferior angle and a downward projection of the anteroinferior angle, this later being somewhat forwardly projected in colobines and baboons. *Lophocebus* is intermediate between these two groups. PC2 mainly separates colobines and baboons. Colobines plot in the positive space of PC2 separately from the other groups of cercopithecids due to their anteroposteriorly wide and mediolaterally flattened parietal regions, combined with a relatively open anteroinferior angle. *Mandrillus*, *Papio*, and *Theropithecus* are to be found in the negative values of PC2 because of their anteroposteriorly narrow and mediolaterally inflated parietal areas.

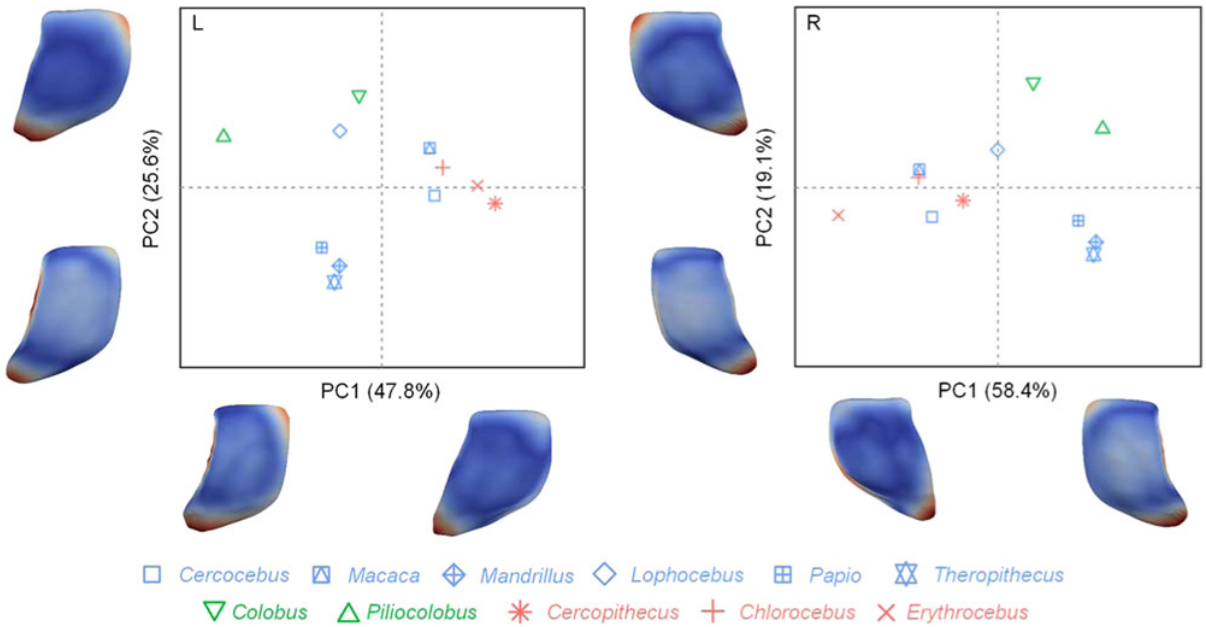

Figure 6. Results from PCA of the isolated left (L) and right (R) parietal surfaces according to the deformation methods. Plots of PC1 vs. PC2 are separated per hemisphere, with the PCA and respective color maps of the left parietal on the left panel, and those of the right parietal on the right panel. The colors on the PCA plot represent the tribes: red, Cercopithecini; blue, Papionini; and green, Colobini. The color maps display the morphological deformations of the parietal surfaces from the grand mean shape to the negative and positive scores of each axis, with the colors indicating the magnitude of displacement (blue: small; red: large)

4. DISCUSSION

Despite the critical role of the parietal lobes in primate evolution and behavior, studies assessing variation in parietal morphology and proportions in the endocasts (and brains) of most primate taxa are still lacking. This might be due to inherent difficulties in locating major anatomical boundaries for digitizing landmarks. Nonetheless, reliable identification of the main sulcal patterns in monkey brains and endocasts is a feasible target (Beaudet et al., 2016; Falk, 1978; Kobayashi et al., 2014; Radinsky, 1974). This is particularly important as endocasts are the only direct evidence of brain anatomy in extinct primate species, and are therefore of prime interest for reconstructing the timing and mode of their cortical evolution. In this study, we compute a comparative neuroanatomical investigation of the cercopithecid parietal lobe shape by quantifying its proportions relative to the whole endocranium, and then compute a specific surface analysis on the parietal region, as to evidence local morphological variations.

4.1. Variation in parietal proportions and shape

One of the purposes of this study was to test whether anatomical differences previously evidenced with descriptive approaches can also be supported through quantitative analysis and to provide quantification of the features involved. By including landmarks located on the main sulci that define the lobes, we attempt to reproduce the previously reported colobine and cercopithecine differences in cortical morphology. According to our landmark set, cercopithecid endocasts vary mostly on the anteroposterior proportions of the parietal and occipital lobes, with colobini exhibiting proportionately larger parietals and cercopithecini larger occipitals. These results are in line with previous descriptive findings on cercopithecid brains (Connolly, 1950) and endocasts (Falk, 1978; Radinsky, 1974), as we found differences between cercopithecinae and colobinae subfamilies. Moreover, our results further evidence

that this difference in proportions is mostly between colobin and cercopithecin tribes since papionins display a larger range of variation in the parietal versus occipital proportions. Indeed, among papionins, *Papio*, and *Theropithecus* display proportions similar to colobins, while the remaining taxa have intermediate values. In addition, our geometric model reveals the second component of variation associated with the height of the parieto-occipital region that might indicate variation in the height of the braincase. Taking into account these two main features (parieto-occipital proportions and braincase height), colobines are characterized by larger parietal lobes and flat endocranial vaults; baboons have larger parietal lobes and tall vaults; cercopithecins display larger occipital lobes and intermediate heights; while *Macaca* and mangabeys tend to exhibit average cercopithecid brain proportions.

The other objective of the present study was to further examine parietal variation by considering the left and right parietal lobe surfaces separately through deformation methods. The results show that the main variation of the parietal surface is associated with the anteroposterior width and mediolateral inflation of the parietal surface, as well as with the configurations of the anteroinferior and posteroinferior angles. The null hypothesis of no morphological differences is hence falsified. These differences in morphology further confirm the larger anteroposterior dimensions of colobine parietals (Connolly, 1950; Falk, 1978; Radinsky, 1974), and indicate mediolateral expansion of the baboon parietal lobes. This latter variation could be due to the larger endocrania of the baboons. In addition, parietal-only variation is also driven by differences in the morphology of sulcal intersections, more specifically, on the junctions between the central sulcus and the lunate sulcus with the inferior parietal limit (Sylvian fissure). The variation on the anteroinferior angle could be explained by a variation on the curvature of the lower portion of the central sulcus, which might be more or less bent among cercopithecids (Connolly, 1950). The variation on the postero-inferior angle, given our methodology for defining the inferior parietal border, i.e., a plane passing through the central sulcus, Sylvian fissure, and lunate sulcus, could be influenced by variation in the extension and patterns of these three sulci. The pattern of the Sylvian fissure and lunate sulcus differ between the two subfamilies. In cercopithecines, the Sylvian fissure is bent and converges with the superior temporal sulcus, and the lunate sulcus is relatively straight, while in colobines, the Sylvian fissure is parallel to the superior temporal sulcus and the lunate sulcus is relatively curved (Falk, 1978). Moreover, baboons seem to display greater variability in their sulcal patterns in general and differ from other cercopithecines in the joint of the intraparietal sulcus with the lunate sulcus, which display a rather right angle (Connolly, 1950).

The variation in parietal versus occipital proportions was generally interpreted as a "displacement" of the lunate sulcus, either anteriorly, increasing the occipital cortex in cercopithecines (Falk, 1978; Radinsky, 1974), or posteriorly, increasing the parietal cortex in colobines (Connolly, 1950). This could indicate changes in the PPC, or more specifically in the superior parietal lobule (SPL; Gonzales, Benefit, McCrossin, & Spoor, 2015). In a study on the midsagittal brain variation among primates, the proportions of the precuneus—the midsagittal portion of the SPL—were found to be fairly preserved across monkeys and apes, though varying intra-specifically to the same extent in both chimpanzees and rhesus macaques (Pereira-Pedro, Rilling, Chen, Preuss, & Bruner, 2017). However, as the cited study included only one of the cercopithecid tribes, Papionini, it would be interesting to perform an additional study on the midsagittal brain variation together with Cercopithecini and Colobini to verify what region of the colobine brain is responsible for those differences.

Variation associated with height probably involves general changes on the braincase rather than localized changes to specific brain lobes, as this variation is only observed in the analysis of relative parietal proportion but not in the parietal-only morphology. Furthermore, changes in height correlate with size. Therefore, it is likely that this component of brain form variation is due to the general cranial architecture, rather than to regional brain cortical differences. Cranial shape variation among papionins seems to be largely influenced by allometry (e.g., Singleton, 2002). The characteristic high vaults of baboons have been reported previously. In a study of the midsagittal brain variation, baboons displayed higher vaults relative to other Papionini (Pereira-Pedro et al., 2017). Moreover, the elevation of the parietal surface was also detected in *Theropithecus* through deformation methods (see the Supporting Information material in Beaudet et al., 2016). Interestingly, the allometric analysis with overall endocranial shape variation indicates a clear deviation of the *Theropithecus*, *Colobus*, and *Piliocolobus*. This is probably due to their smaller relative brain sizes compared with similar-sized taxa, which in turn has been associated with their herbivorous diet (Clutton-Brock & Harvey, 1980; Gonzales et al., 2015).

4.2. Limitations and methodological considerations

The main limit of this study regards the reduced sample size. Our sample is composed of 30 specimens spanning 11 genera, which results in some genera including only a few individuals. Further analyses on endocranial anatomy should be based on larger samples, and include a larger number of specimens within each genus. Other authors have recommended avoiding mixing males and females, for instance, in analyses of volume variation (Isler et al., 2008) and sulcal length asymmetry (Imai, Sawada, Fukunishi, Sakata-Haga, & Fukui, 2011). However, in the case of sulcal patterns, mixing males and females should have no influence on the results, as sex differences do not exceed individual variability (Connolly, 1950).

In general, the distribution of the genera in the shape space is similar in both methods, with the genera being roughly separated by the main tribes predominantly driven by the dimensions of the parietal lobe. However, it is important to note that the two methodological approaches are intrinsically distinct as they are based on different types of data (landmarks vs. surface) and target different information, and thus should be regarded as complementary. The landmark analysis is meant to provide information on parietal variation relative to the whole brain (endocast), i.e., in terms of proportional changes, while the surface deformation analysis was used to gain further insight into the local variation that cannot be captured by landmarks. This study constitutes the first attempt to isolate the parietal surface from endocasts. Results suggest that our approach to extract the parietal region can be useful to investigate the parietal variation, and can also give some insights into variation of sulcal patterns. Nonetheless, it must be taken into account that this is only possible when using specimens in which the traces of the cortical sulci can be distinguished on the endocast, which would be difficult in larger primate species with smoother sulcal imprints.

4.3. Implications for cercopithecid parietal evolution

The differences in parietal and occipital lobe proportions among cercopithecoids could result from the evolutionary expansion of either the occipital cortex in cercopithecini or the parietal cortex in colobini and baboons. Previous research has focused on the evolution of the occipital cortex, given the contribution of vision to primate brain evolution (Kirk, 2006). For instance, it has been shown that specific visual mechanisms have increased with encephalization in primates, particularly those associated with the analysis of fine detail and

color, processed by the parvocellular system of the lateral geniculate nucleus (Barton, 1998). Cercopithecines display six parvocellular layers, while some colobines have fewer, which might be associated with differences in visual processing (de Sousa, Sherwood, Hof, & Zilles, 2013). In macaques, about 55% of the neocortex is visual in function (Felleman & Van Essen, 1991), and the volume of the primary visual cortex increases rapidly with brain size (de Sousa et al., 2010). Larger primary visual cortex can process more information and represent the visual field with more detail, thus increasing visual acuity (de Sousa & Proulx, 2014). However, the visual areas are not only restricted to the occipital lobes (Felleman & Van Essen, 1991), and the larger primary visual cortex might also indicate an increase in connectivity (de Sousa & Proulx, 2014). Moreover, the relatively smaller colobine occipital lobes do not explain why their parietal lobes are larger.

According to Strasser and Delson (1987), most of the anatomical characters distinguishing colobines and cercopithecines are associated with either dietary specializations or locomotor behavior. Visuospatial integration and eye-hand coordination, functions that are essential both for locomotion and feeding behaviors, are processed within the parietal cortex. For instance, the posterior parietal cortex is undoubtedly involved in various forms of visuospatial processing (Kravitz, Saleem, Baker, & Mishkin, 2011), and is part of the dorsal visual stream, integrating identification and spatial location of objects and information on the movement type and part of the body performing it (Freud, Plaut, & Behrmann, 2016). It ultimately has a role in manual dexterity, a distinctive feature of primates (Ross & Martin, 2007).

Gonzales et al. (2015) associated the expansion of colobine SPL to their specialized folivorous diet, specifically to reaching and grasping functions (Bakola, Gamberini, Passarelli, Fattori, & Galletti, 2010; Hadjidimitrakis, Breveglieri, Bosco, & Fattori, 2012) needed for picking up leaves. However, all cercopithecids use their hands to reach and grasp their food, and, as our results show, *Papio* also tend to have proportionately larger parietals, on average, despite being omnivores.

According to van Schaik, Deaner, and Merrill (1999), most of the highly-dexterous genera show tool to use for feeding. Considering only the genera within our study, they observed complex manipulation and use of tools for feeding (mostly in captivity) among *Cercopithecus*, *Erythrocebus*, *Macaca*, *Cercocebus*, *Papio*, and *Mandrillus. Theropithecus*, in spite of showing complex manipulation, does not use feeding tools. *Colobus* shows neither hand dexterity nor use of tools. Colobines have a particular hand morphology, characterized by evolutionary reduction, or loss, in the case of *Colobus*, of the thumb (Frost, Gilbert, Pugh, Guthrie, & Delson, 2015; Strasser & Delson, 1987), which is regarded as an adaptation to arboreal life (e.g., Nakatsukasa et al., 2010). In contrast, *Theropithecus* and *Cebus* convergently evolved hand proportions similar to those of humans, with short lateral digits and longer thumbs relative to digits (Almécija, Smaers, & Jungers, 2015). This hand morphology, typical of terrestrial quadruped primates, is compatible with opposable thumbs, and enhances complex manipulation, as in baboons and geladas (Heldstab et al., 2016). Besides substrate use, the evolution of hand dexterity and complex manipulation in primates required changes within the brain (Heldstab et al., 2016), which might have involved an extension of the PPC and somatosensory cortex (Almécija & Sherwood, 2017). It would be interesting to investigate the cortical differences in somatosensory representations between colobines and cercopithecines.

Interestingly, among the New World monkeys, the genus *Cebus* seems to have independently evolved some cercopithecid traits, namely, a similar sulcal pattern (Connolly, 1950; Gonzales et al., 2015), and an opposable thumb, coupled with the ability to use tools for feeding (Goldring & Krubitzer, 2017; Padberg et al., 2007). Padberg et al. (2007) suggested that the emergence of parietal cortical areas involved in skilled hand use in New and Old World monkeys is an outcome of the development of similar hand morphology and use in both families. Including *Cebus* specimens in our analysis would add invaluable information concerning the variation of the parietal lobe anatomy and proportions.

Larger parietal proportions are displayed by Colobines, *Theropithecus*, and *Papio*, which have distinct ecological niches, diets, and locomotion. Therefore, gross morphological brain variations are likely to be due to distinct aspects, and not only influenced by shared ecological factors. In this context, the evolution of large parietal independently in colobines and baboons cannot be ruled out. Aristide et al. (2016) observed significant convergence in overall endocranial shape in different platyrrhine families. Moreover, factors other than ecology could have played a role in parietal evolution. For instance, Falk (1981) associated the anterior displacement of the arcuate sulcus in geladas to an expansion of the somato-motor face representation due to their ability to retract the lip. Additional studies should consider variation in cytoarchitecture and functional parcellation within the parietal cortex to fully understand which roles contributed the most to the variation in the proportion of this lobe within cercopithecids. For instance, it would be interesting to investigate the cytoarchitectonic and functional changes within the parietal cortex in species with rudimentary thumbs in contrast to species with opposable thumbs, especially considering the areas containing a topographic map of the body parts (Padberg et al., 2007).

ACKNOWLEDGMENTS

For their technical and/or scientific discussion/collaboration, we are grateful to J. Braga (Toulouse), S. Durrleman (Paris), J. Dumoncel (Toulouse), D. Stratford (Johannesburg), G. Subsol (Montpellier). We are indebted to J. Cuisin (Paris), G. Fleury (Toulouse), E. Gilissen and W. Wendelen (Tervuren) for having granted access to material under their care. We also thank C. Tenailleau and B. Duployer (Toulouse), G. Clément, and M. Garcia-Sanz (Paris) for the microtomographic acquisitions. This study was supported by the Italian Institute of Anthropology, and by a travel fellowship approved by Universidad de Burgos (Spain). ASPP is funded by Fundación Atapuerca. AB is funded by the Claude Leon Foundation and by the Centre of Excellence in Palaeosciences. EB is funded by Ministerio de Ciencia, Innovación y Universidades PGC2018-093925-B-C31). The authors would like to thank the Centre for High-Performance Computing (CHPC) in South Africa for granting access to the computational resources used in this work.

CONFLICT OF INTERESTS

The authors declared that there is no conflict of interests.

REFERENCES

Almécija, S., & Sherwood, C. C. (2017). Hands, brains, and precision grips: Origins of tool use behaviors. In L. Krubitzer, & J. H. Kaas (Eds.), Evolution of Nervous Systems, Volume 3: The Nervous System of Non-HumanPrimates (pp. 299– 315). Elsevier Academic Press.

Almécija, S., Smaers, J. B., & Jungers, W. L. (2015). The evolution of human and ape hand proportions. *Nature Communications*, 6, 7717. https://doi-org/10.1038/ncomms8717

Aristide, L., dos Reis, S. F., Machado, A. C., Lima, I., Lopes, R. T., & Perez, S. I. (2016). Brain shape convergence in the adaptive radiation of New World monkeys. *Proceedings of the National Academy of Sciences*, 113(8), 2158– 2163. https://doi-org/10.1073/pnas.1514473113

Bakola, S., Gamberini, M., Passarelli, L., Fattori, P., & Galletti, C. (2010). Cortical connections of parietal field PEc in the macaque: Linking vision and somatic sensation for the control of limb action. *Cerebral Cortex*, 20(11), 2592– 2604. https://doi-org/10.1093/cercor/bhq007

Barton, R. A. (1998). Visual specialization and brain evolution in primates. *Proceedings of the Royal Society of London. Series B: Biological Sciences*, 265, 1933– 1937. https://doi-org/10.1098/rspb.1998.0523

Beaudet, A., & Bruner, E. (2017). A frontal lobe surface analysis in three African human fossils: OH 9, Buia, and Bodo. *Comptes Rendus Palevol*, 16, 499– 507. https://doi-org/10.1016/j.crpv.2016.12.002

Beaudet, A., Dumoncel, J., deBeer, F., Duployer, B., Durrleman, S., Gilissen, E., … Braga, J. (2016). Morphoarchitectural variation in South African fossil cercopithecoid endocasts. *Journal of Human Evolution*, 101, 65– 78. https://doi-org/10.1016/j.jhevol.2016.09.003

Beaudet, A., Dumoncel, J., deBeer, F., Durrleman, S., Gilissen, E., Oettlé, A., … Braga, J. (2018). The endocranial shape of *Australopithecus africanus*: Surface analysis of the endocasts of Sts 5 and Sts 60. *Journal of Anatomy*, 232(2), 296– 303. https://doi-org/10.1111/joa.12745

Bruner, E. (2018). The brain, the braincase, and the morphospace. In E. Bruner, N. Ogihara, & H. C. Tanabe (Eds.), Digital Endocasts: from skulls to brains (pp. 93– 114). Japan: Springer.

Bruner, E., & Iriki, A. (2016). Extending mind, visuospatial integration, and the evolution of the parietal lobes in the human genus. *Quaternary International*, 405(A), 98– 110. https://doi-org/10.1016/j.quaint.2015.05.019

Catani, M., Robertsson, N., Beyh, A., Huynh, V., deSantiago Requejo, F., Howells, H., … Dell'Acqua, F. (2017). Short parietal lobe connections of the human and monkey brain. *Cortex*, 97, 339– 357. https://doi-org/10.1016/j.cortex.2017.10.022

Clutton-Brock, T. H., & Harvey, P. H. (1980). Primates, brains, and ecology. *Journal of Zoology*, 190(3), 309– 323. https://doi-org/10.1111/j.1469-7998.1980.tb01430.x

Connolly, C. J. (1950). External morphology of the primate brain. Springfield Illinois: Charles C. Thomas.

Copes, L. E., Lucas, L. M., Thostenson, J. O., Hoekstra, H. E., & Boyer, D. M. (2016). A collection of nonhuman primate computed tomography scans housed in MorphoSource, a repository for 3D data. *Scientific Data*, 3, 160001. https://doi-org/10.1038/sdata.2016.1

Dupej, J., Rangel de Lázaro, G., Pereira-Pedro, A. S., Pisová, H., Pelikán, J., & Bruner, E. (2018). Comparing endocranial surfaces: Mesh superimposition and coherent point drift registration. In E. Bruner, N. Ogihara, & H. C. Tanabe (Eds.), Digital Endocasts: From skulls to brains (pp. 143– 152). Japan: Springer.

Durrleman, S., Pennec, X., Trouvé, A., Ayache, N., & Braga, J. (2012). Comparison of the endocranial ontogenies between chimpanzees and bonobos via temporal regression and spatiotemporal registration. *Journal of Human Evolution*, 62(1), 74– 88. https://doi-org/10.1016/j.jhevol.2011.10.004

Durrleman, S., Prastawa, M., Charon, N., Korenberg, J. R., Joshi, S., Gerig, G., … Trouvé, A. (2014). Morphometry of anatomical shape complexes with dense deformations and sparse parameters. *NeuroImage*, 101, 35– 49. https://doi-org/10.1016/j.neuroimage.2014.06.043

Falk, D. (1978). Brain evolution in old World monkeys. *American Journal of Physical Anthropology*, 48(3), 315– 319. https://doi-org/10.1002/ajpa.1330480307

Falk, D. (1981). Sulcal patterns of fossil *Theropithecus* baboons: Phylogenetic and functional implications. *International Journal of Primatology*, 2(1), 57– 69. https://doi-org/10.1007/BF02692300

Felleman, D. J., & VanEssen, D. C. (1991). Distributed hierarchical processing in the primate cerebral cortex. *Cerebral Cortex*, 1, 1– 47. https://doi-org/10.1093/cercor/1.1.1

Freud, E., Plaut, D. C., & Behrmann, M. (2016). 'What' is happening in the dorsal visual pathway. *Trends in Cognitive Sciences*, 20(10), 773– 784. https://doi-org/10.1016/j.tics.2016.08.003

Frost, S. R., Gilbert, C. C., Pugh, K. D., Guthrie, E. H., & Delson, E. (2015). The hand of *Cercopithecoides williamsi* (Mammalia, Primates): Earliest evidence for thumb reduction among colobine monkeys. *PLoS One*, 10(5), e0125030. https://doi-org/10.1371/journal.pone.0125030

Goldring, A. B., & Krubitzer, L. A. (2017). Evolution of parietal cortex in mammals: From manipulation to tool use. In L. Krubitzer, & J. H. Kaas (Eds.), Evolution of Nervous Systems, Volume 3: The Nervous System of Non-Human Primates (pp. 259– 286). Elsevier.

Gonzales, L. A., Benefit, B. R., McCrossin, M. L., & Spoor, F. (2015). Cerebral complexity preceded enlarged brain size and reduced olfactory bulbs in Old World monkeys. *Nature Communications*, 6, 7580. https://doi-org/10.1038/ncomms8580

Grefkes, C., & Fink, G. R. (2005). The functional organization of the intraparietal sulcus in humans and monkeys. *Journal of Anatomy*, 207(1), 3– 17. https://doi-org/10.1111/j.1469-7580.2005.00426.x

Grubb, P., Butynski, T. M., Oates, J. F., Bearder, S. K., Disotell, T. R., Groves, C. P., … Struhsaker, T. T. (2003). Assessment of the diversity of African primates. *International Journal of Primatology*, 24(6), 1301– 1357. https://doi-org/10.1023/B:IJOP.0000005994.86792.b9

Hadjidimitrakis, K., Breveglieri, R., Bosco, A., & Fattori, P. (2012). Three-dimensional eye position signals shape both peripersonal space and arm movement activity in the medial posterior parietal cortex. *Frontiers in Integrative Neuroscience*, 6, 37. https://doi-org/10.3389/fnint.2012.00037

Hammer, Ø., Ryan, P., & Harper, D. (2001). PAST: Paleontological statistics software package for education and data analysis. *Palaeontologia Electronica*, 4(1), 1– 9. https://doi-org/10.1.1.459.1289

Heldstab, S. A., Kosonen, Z. K., Koski, S. E., Burkart, J. M., vanSchaik, C. P., & Isler, K. (2016). Manipulation complexity in primates coevolved with brain size and terrestriality. *Scientific Reports*, 6, 24528. https://doi-org/10.1038/srep24528

Imai, N., Sawada, K., Fukunishi, K., Sakata-Haga, H., & Fukui, Y. (2011). Sexual dimorphism of sulcal length asymmetry in the cerebrum of adult cynomolgus monkeys (*Macaca fascicularis*). *Congenital Anomalies*, 51(4), 161– 166. https://doi-org/10.1111/j.1741-4520.2011.00330.x

Isler, K., Christopher Kirk, E., Miller, J. M. A., Albrecht, G. A., Gelvin, B. R., & Martin, R. D. (2008). Endocranial volumes of primate species: Scaling analyses using a comprehensive and reliable data set. *Journal of Human Evolution*, 55(6), 967– 978. https://doi-org/10.1016/j.jhevol.2008.08.004

Jolliffe, I. T. (2002). Principal Component Analysis (2nd ed.). New York, NY: Springer.

Kastner, S., Chen, Q., Jeong, S. K., & Mruczek, R. E. B. (2017). A brief comparative review of primate posterior parietal cortex: A novel hypothesis on the human toolmaker. *Neuropsychologia*, 105, 123– 134DOI: 0.1016/j.neuropsychologia.2017.01.034

Kirk, E. C. (2006). Visual influences on primate encephalization. *Journal of Human Evolution*, 51, 76– 90. https://doi-org/10.1016/j.jhevol.2006.01.005

Klingenberg, C. P. (2011). MorphoJ: An integrated software package for geometric morphometrics. *Molecular Ecology Resources*, 11(2), 353– 357. https://doi-org/10.1111/j.1755-0998.2010.02924.x

Klingenberg, C. P., Barluenga, M., & Meyer, A. (2002). Shape analysis of symmetric structures: Quantifying variation among individuals and asymmetry. *Evolution; International Journal of Organic Evolution*, 56(10), 1909– 1920. https://doi-org/10.1111/j.0014-3820.2002.tb00117

Kobayashi, Y., Matsui, T., Haizuka, Y., Ogihara, N., Hirai, N., & Matsumura, G. (2014). Cerebral sulci and gyri observed on macaque endocasts. In T. Akazawa, N. Ogihara, H. C. Tanabe, & H. Terashima (Eds.), Dynamics of Learning in Neanderthals and Modern Humans, Volume 2: Cognitive and Physical Perspectives (pp. 131– 137). Japan: Springer.

Kravitz, D. J., Saleem, K. S., Baker, C. I., & Mishkin, M. (2011). A new neural framework for visuospatial processing. *Nature Reviews Neuroscience*, 12(4), 217– 230. https://doi-org/10.1038/nrn3008

VanMinh, N., & Hamada, Y. (2017). Age-related changes of sulcal imprints on the endocranium in the Japanese macaque (*Macaca fuscata*). *American Journal of Physical Anthropology*, 163(2), 285– 294. https://doi-org/10.1002/ajpa.23205

Nakatsukasa, M., Mbua, E., Sawada, Y., Sakai, T., Nakaya, H., Yano, W., … Kunimatsu, Y. (2010). Earliest colobine skeletons from Nakali, Kenya. *American Journal of Physical Anthropology*, 143(3), 365– 382. https://doi-org/10.1002/ajpa.21327

Neubauer, S. (2014). Endocasts: Possibilities and limitations for the interpretation of human brain evolution. *Brain, Behavior, and Evolution*, 84(2), 117– 134. https://doi-org/10.1159/000365276

Padberg, J., Franca, J. G., Cooke, D. F., Soares, J. G. M., Rosa, M. G. P., Fiorani, M., … Krubitzer, L. (2007). Parallel evolution of cortical areas involved in skilled hand use. *Journal of Neuroscience*, 27(38), 10106– 10115. https://doi-org/10.1523/JNEUROSCI.2632-07.2007

Pereira-Pedro, A. S., & Bruner, E. (2018). Landmarking endocasts. In E. Bruner, N. Ogihara, & H. C. Tanabe (Eds.), Digital Endocasts: From skulls to brains (pp. 127– 142). Japan: Springer.

Pereira-Pedro, A. S., Rilling, J. K., Chen, X., Preuss, T. M., & Bruner, E. (2017). Midsagittal brain variation among nonfuman primates: Insights into evolutionary expansion of the human precuneus. *Brain, Behavior, and Evolution*, 90(3), 255– 263. https://doi-org/10.1159/000481085

Radinsky, L. (1974). The fossil evidence of anthropoid brain evolution. *American Journal of Physical Anthropology*, 41(1), 15– 27. https://doi-org/10.1002/ajpa.1330410104

Ross, C. F., & Martin, R. D. (2007). The role of vision in the origin and evolution of primates. In T. M. Preuss (Ed.), The Evolution of Nervous Systems, Volume 4: Primates (pp. 59– 78). Oxford: Elsevier.

vanSchaik, C. P., Deaner, R. O., & Merrill, M. Y. (1999). The conditions for tool use in primates: Implications for the evolution of material culture. *Journal of Human Evolution*, 36(6), 719– 741. https://doi-org/10.1006/jhev.1999.0304

Singleton, M. (2002). Patterns of cranial shape variation in the Papionini (Primates: Cercopithecinae). *Journal of Human Evolution*, 42(5), 547– 578. https://doi-org/10.1006/jhev.2001.0539

deSousa, A. A., & Proulx, M. J. (2014). What can volumes reveal about human brain evolution? A framework for bridging behavioral, histometric, and volumetric perspectives. *Frontiers in Neuroanatomy*, 8, 51. https://doi-org/10.3389/fnana.2014.00051

deSousa, A. A., Sherwood, C. C., Hof, P. R., & Zilles, K. (2013). Lamination of the lateral geniculate nucleus of catarrhine primates. *Brain, Behavior, and Evolution*, 81, 93– 108. https://doi-org/10.1159/000346495

deSousa, A. A., Sherwood, C. C., Mohlberg, H., Amunts, K., Schleicher, A., MacLeod, C. E., … Zilles, K. (2010). Hominoid visual brain structure volumes and the position of the lunate sulcus. *Journal of Human Evolution*, 58, 281– 292. https://doi-org/10.1016/j.jhevol.2009.11.011

Strasser, E., & Delson, E. (1987). Cladistic analysis of cercopithecid relationships. *Journal of Human Evolution*, 16(1), 81– 99. https://doi-org/10.1016/0047-2484(87)90061-3

Subsol, G., Gesquière, G., Braga, J., & Thackeray, F. (2010). 3D automatic methods to segment 'virtual' endocasts: State of the art and future directions. *American Journal of Physical Anthropology*, 141(Suppl. 50), 226– 227.

Whitlock, J. R. (2017). Posterior parietal cortex. *Current Biology*, 27(14), R691– R695. https://doi-org/10.1016/j.cub.2017.06.007

Zelditch, M. L., Swiderski, D. L., Sheets, H. D., & Fink, W. L. (2004). Geometric Morphometrics for Biologists. New York and London: Elsevier Academic Press.